U.P.B. Sci. Bull., Series B, Vol. 76, Iss. 1, 2014 ISSN 1454 – 2331

FAC AND *MER*- AlQ_3 ISOMERS OBTAINED BY DIRECT SOLID STATE REACTION

Iulia Corina CIOBOTARU[1], Silviu POLOSAN[2], Horia IOVU[3]

A new route for AlQ_3 synthesis was developed starting from $Al(OH)_3$ and 8-hydroxyquinoline compounds, by solid state reaction. At 95°C the bayerite and/or gippsite of $Al(OH)_3$ is decomposed in AlO(OH) boemite which react with 8-hydroxyquinoline, leading to a new crystalline phase containing both meridional and facial Alq_3 isomers. Vibrational spectroscopy gives useful details for identification of fac and mer isomers. X-ray diffraction patterns confirm the presence of a triclinic structure with low symmetry. Scanning Electron Microscopy and cathodoluminescence measurements confirm the presence of an unstable compound under the electron beam and characteristic X-ray with lower emission efficiency.

Keywords: *Tris* (8-hydroxyquinoline) aluminum, OLED, solid state reaction

1. Introduction

Tris (8-hydroxyquinoline) aluminum is an organometallic molecule widely used in different areas, especially in the light emitting layer for the Organic Light Emitting Diodes (OLED`s) [1-5] but also as an electron transport layer [6,7], host for fluorescent and phosphorescent dyes [8,9].

Alq_3 is an octahedrally coordinated chelate complex $M(N\^{}O)_3$, where M is a trivalent metal, N and O are the nitrogen and oxygen atoms in the bidentate quinolinolate ligand. The Alq_3 complex can occur in two isomeric forms (facial and meridional), depending on the orientations of the ligands [10].

Beside of these two isomers, the thermal annealing processes induces different crystalline structures called α, β, γ and even δ phase [11]. These phases can be determined from Differential Scanning Calorimetry (DSC) starting with 290°C up to 420°C where the melting point is [12].

Several efforts have been made to prepare both isomers and for tuning the emission wavelength of Alq_3 through modulation of HOMO levels, by synthesizing differently substituted 8-hydroxyquinolines in which the

---

[1] PhD Student, Group of Functional Nanostructures, National Institute of Materials Physics, Romania, e-mail: cora.radu@yahoo.com

[2] Senior Researcher II, Group of Functional Nanostructures, National Institute of Materials Physics, Romania.

[3] Prof., Advanced Polymer Materials Group, University POLITEHNICA of Bucharest, Romania

substitutions are introduced to the phenoxide ring [13]. Various other aspects, such as doping electroluminescent materials into Alq_3 [14], or by embedding Alq_3 into mesoporous materials [15] have been studied. In parallel, different types of Alq_3 with variety of field-emission properties were investigated and reported as nanoparticle [16], wirelike [17] and blue luminescent δ crystal phase Alq_3 [18–20].

The common way to prepare the Alq_3 compounds is the wet synthesis in which 8-hydroxyquinoline is mixed with different aluminum salts like $AlCl_3$, $Al(OH)_3$, $Al(NO_3)_39H_2O$ or $Al_3(SO_4)_3nH_2O$, which provide mainly meridional isomer or α-phase [21]. Comparing the luminescence of δ-phase and α-phase, there is a blue shift of about 0.2 eV [19]. It is generally agreed that the meridional form of Alq_3 is predominant in the both amorphous and crystalline structures. Another route to obtain different crystalline phases, except the α-phase, is thermal sublimation of the α-Alq_3.

The aim of this paper is to develop a new route for synthesis of Alq_3 by pure solid state reaction (further called solid state reaction compound or ssr) between 8-hydroxyquinoline and $Al(OH)_3$. Previous attempts have been made by using the solid state reaction between aluminum oxide-hydroxide $AlO(OH)$ with 8-hydroxyquinoline but in a different way [21]. Due the water insolubility of the $AlO(OH)$, the synthesis with 8-hydroxyquinoline was done by mixing the compound in the demineralized water and stirred under reflux in an oil bath maintained at 110^{o}C.

Several measurement techniques have been involved in characterization of the mer-Alq_3 and the new compound like Differential Scanning Calorimetry (DSC), X-ray diffraction (XRD), photoluminescence, Raman and FT-IR vibrational spectroscopy, SEM and cathodoluminescence measurements.

2. Materials and methods

Solid state reaction was done by mixing 8-hydroxyquinoline and $Al(OH)_3$ in quartz crucible, in the ratio 2:1 in order to compare the final compound with the most common *mer*-Alq_3. The mixture was then slowly milled until the homogeneity was reached. The quartz crucible was moved in the Nabertherm programmable furnace and heated up to 95^{o} C with a 10^{o}/min. and kept for 36 hours in air. The cooling was done in air by slow quenching of the obtained compound. The final powder is pale yellowish colored.

Meridional tris (8-hydroxyquinoline) aluminum (Alq_3) was synthesized by mixing 8-hydroxyquinoline and $Al(OH)_3$ at about 95°C. In a typical synthesis, 0.39 g (0.005 mol) of $Al(OH)_3$ was gradually dropped into 80 ml distilled water which contains 1.45 g (0.01 mol) of 8-hydroxyquinoline. The ratio between 8-hydroxyquinoline and $Al(OH)_3$ was chosen as 2:1, which in the fast reaction conditions (up to 24 h), results in the *mer*-Alq$_3$ formation. When this ratio is 3:1, the synthesis leads to the formation of needle-shape of 8-quinolinol crystals [22]. The pH was adjusted by using acetic acid in order to dissolve the 8-hydroxyquinoline powder. The reaction time of 6 h led to the production of yellowish Alq$_3$ powder. In the final stage, the pH was adjusted to the neutral value by adding NH$_3$ (precipitating agent) drop by drop with continuous stirring to get the maximum yield. The synthesized Alq$_3$ is obtained as a form of precipitate.

This precipitate was filtered and washed with double distilled water until the filtered became colorless and dried at 110 °C for 10 days. From the synthesis, the raw powder has partially crystalline structure. The powder consists of a very large number of randomly oriented micro-size crystals or particles.

2.1. Advanced characterization

For the Differential Scanning Calorimetry (DSC), we have used a SETARAM Setsys Evolution 18 in TG-DSC mode Thermal Analyzer in the 25 to 400 °C temperature range.

The XRD measurements have been performed on a BRUKER D8 ADVANCE type X-ray diffractometer, in focusing geometry, equipped with copper target X-ray tube and LynxEye one-dimensional detector, using CuK$_{\alpha 1}$ radiation (λ = 1.54056 Å), at 40 kV and 40 mA. The 2θ scan range was 5–20°, with a step size of 0.02° and 0.01° resolution. The XRD patterns were obtained after subtraction of K$_{\alpha 2}$ lines from the K$_{\alpha 1}$-K$_{\alpha 2}$ doublet, by the Rachinger algorithm, using the Bruker Difrac^{plus} Basic Evaluation program package [23].

We employed a Zeiss EVO 50 SEM with LaB$_6$ cathode with Brucker EDX system. Based on the SEM images, the equipment can generate secondary electrons, back scattered electrons, characteristic X-ray and cathodoluminescence.

Raman spectra have been recorded on bulk glass samples with a Jasco NRS-3100 spectrometer, from 50 to 1000 cm^{-1}, using 632 nm lasers. Infrared spectra have been recorded at room temperature with a Jasco FT-IR FT/IR-6200 type A spectrometer with a TGS detector, between 7000-350 cm^{-1}. The scan speed was set at 2 mm/s and the resolution at 2 cm^{-1}. Photoluminescence (PL) spectra have been recorded at room temperature, in the UV-VIS region 200-800 nm, using Edinburgh F900 spectrophotometer.

Molecular geometry of *mer*-Alq$_3$ and *fac*-Alq$_3$ were optimized using Kohn-Sharm Density Functional Theory (DFT) [24] and computational calculations with Gaussian 03W software.

We have used the B3LYP hybrid exchange correlation functional of Becke three-parameter theory and 6-31g basic sets, including geometry connectivity. After initial geometry optimization, the next steps of calculation were dedicated to Raman and infrared computational spectra for the both isomers.

3. Results and discussion.

3.1. Differential Scanning Calorimetry Analysis

Thermal decomposition of $Al(OH)_3$ can be evaluated by DSC measurements from 20 to 400°C. Figure 1 shows the results of DSC curves of the initial $Al(OH)_3$ and the compound obtained by solid state reaction.

On the initial DSC curve, a large endotermic peak centered at 170° C, is observed between 50 to 350°C. This decomposition peak of aluminum hydroxide involves the following evolution of phases [25]:

$$Al(OH)_3 \rightarrow AlO(OH)$$

In other words, the bayerite and/or gippsite structure of $Al(OH)_3$ suffer a partial water loss and is transformed in boehmite. The small endothermic peak from 40°C can be assigned to the loss of water surface from the $Al(OH)_3$ crystals.

When the solid state reaction between $Al(OH)_3$ and 8-hydroxyquinoline take place, the endothermic peak from 170°C strongly decreases and an exothermic peak centered at 380°C with a long tail up to 390°C appears. The solid state reaction process was made at fixed temperature (95°C) in order to compare the powder with the wet chemical synthesis of *mer*-Alq_3, made at the same temperature.

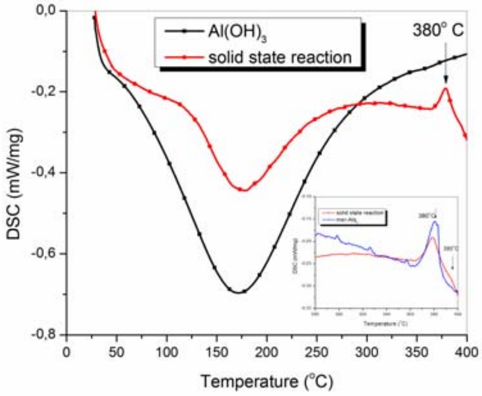

Fig. 1. Differential Scanning Calorimetry before and after solid state reaction

3.2. X-Ray Diffraction Analysis

Rajeswaran et al. [26] have studied the phase changing of α-Alq_3 from 20 to 440, and found two exothermic peak centered at 389° C, and 405° C, but with 50°C/min. which were attributed to γ and δ Alq_3 phases. In our case, using a scan speed of 10°C/min., these two peaks appear at 380°C and 395°C (see the inlet). In the *mer*-Alq_3, the second peak is not so prominent, suggesting a lower δ-phase concentration, compared with the new compound obtained by solid sate reaction.

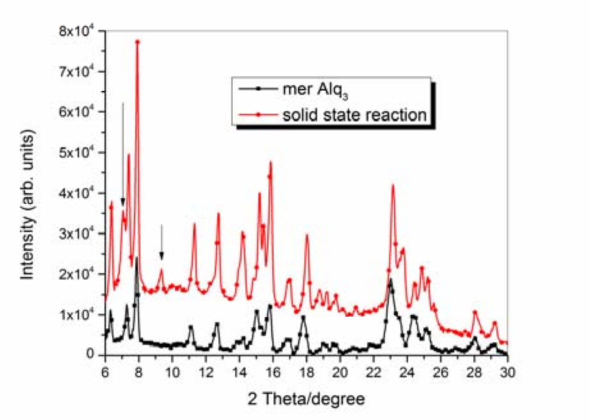

Fig. 2. X-ray diffraction patterns of *mer*-Alq_3 and solid state reaction compound.

A comparison between the XRD patterns of *mer*-Alq_3 and the solid state reaction product reveals some significant differences (figure 2). Firstly is the presence of a new peak at $2\theta=7.05^{\circ}$. Similar behavior was observed by M. Cölle et al. and was assigned to the blue Alq_3, obtained from the yellowish-green Alq_3 powder (α-Alq3) which was annealed at 400°C for 2 h and at 410°C for a few minutes [10]. Secondly, in the solid state reaction product, some additional peaks between 22° and 26° appears, especially the one at 25.8°. Similar behaviors were observed by M. Cölle et al. when the annealing has been done at 390° C, besides the peak from 7.05°. All of these characteristics were attributed to the δ-Alq_3 which has a blue emission as we will see in the photoluminescence measurements. However, the presence of one peak at 9.35°, which is due to the un-reacted 8-hydroxyquinoline, denote an incomplete reaction.

3.3.Raman Spectroscopy

Vibrational spectroscopy allow us to show the formation of the Alq3 powder (mer and/or fac isomers) and gives useful details about the structure of the Alq_3 in order to indentify each isomer contribution.

In the figure 3, it is a comparison between the Raman behaviors of the pale yellowish powder obtained by solid state reaction, the *mer*-Alq_3 compound and the 8-hydroxyquinoline.

This figure and the inlet, shows only the main differences which appears at low frequencies (below 150 cm^{-1}) and at 525-550 cm^{-1}. Both zones give useful details about the Al-O and Al-N vibrations. At low frequencies, mer-Alq_3 shows three peaks centered at 70 cm^{-1} and 99 cm^{-1} which were attributed to the Al-O vibrations, called Al-oxine deformations [26].

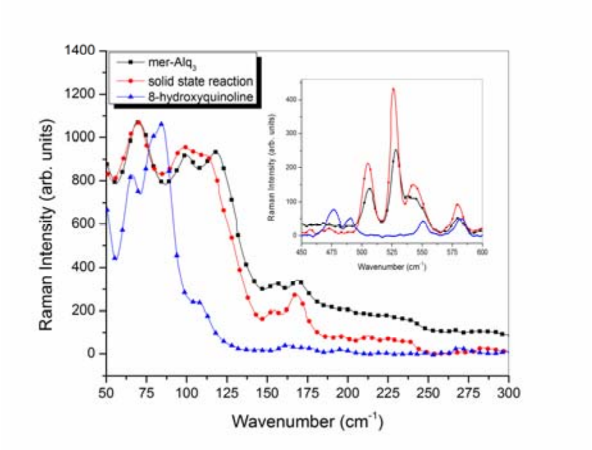

Fig. 3. Comparison between Raman spectra of *mer*-Alq_3, 8-hydroxiquinoline and the solid state reaction compound.

Another broad peak at 118 cm^{-1} and 124 cm^{-1} shoulder was reasonably assigned to the coupled vibrations Al–O deformation + Al-N stretching and C-O-Al bending. In the case of the compound obtained by solid state reaction, the C-O-Al bending seems to be in the same position, around 124 cm^{-1}, but the main peak is shifted from 118 cm^{-1} to 113 cm^{-1}. It means that the above coupled vibrations have slightly different Al-O and Al-N bonding lengths.

In the second vibrational zone, from 525 cm^{-1} and 550 cm^{-1}, there are three predicted peaks in mer-Alq_3 at 525 cm^{-1}, 534 cm^{-1} and 541 cm^{-1}. The first peak was assigned to the coupled vibrational modes Al-O stretching and ring deformation [26]. The other two peaks comes from another coupled modes formed by Al-O and Al-N stretching, and ring deformation. In our case, a broad peak centered at 539 cm^{-1} with a shoulder at 545 cm^{-1} can be seen. It is supposed that in the case of the compound obtained by solid state reaction, some Al-O and Al-N vibrations are altered probably due to the configurationally changes between compounds. The last vibrational peak from 549 cm^{-1} comes from the 8-hydroxyquinoline vibrations.

3.4. FT-IR Analysis

Figure 4 shows the IR spectra of *mer*-Alq_3 in comparison with the compound obtained by solid state reaction, both powders being spread on the KRS glass to ensure the transparency in the whole IR range. The inlet shows the peak shift assigned to the coupled vibrations between Al-O and Al-N stretching and ring deformation. Although both spectra have almost the same peak positions, some differences can be evidenced between powders. The *mer*-Alq$_3$ compound reveals two peaks centered at 648 cm^{-1} and 547 cm^{-1} that corresponds to the Al-O stretching modes [28].

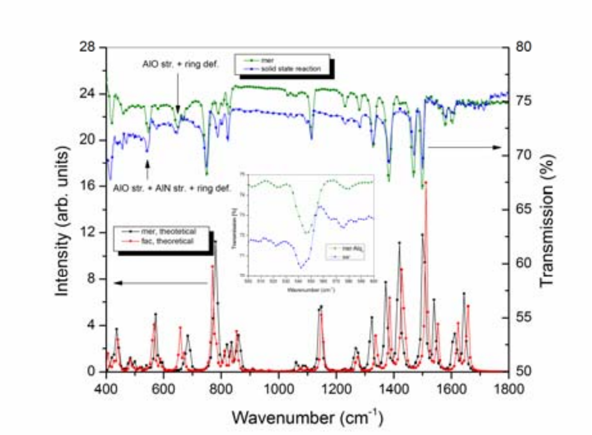

Fig. 4. FT-IR spectra of *mer*-Alq$_3$ and the solid state reaction compound together with DFT results

Figure 4 shows the IR spectra of *mer*-Alq$_3$ in comparison with the compound obtained by solid state reaction, both powders being spread on the KRS glass to ensure the transparency in the whole IR range. The inlet shows the peak shift assigned to the coupled vibrations between Al-O and Al-N stretching and ring deformation. Although both spectra have almost the same peak positions, some differences can be evidenced between powders. The *mer*-Alq$_3$ compound reveals two peaks centered at 648 cm^{-1} and 547 cm^{-1} that corresponds to the Al-O stretching modes [28]. More precisely, the first peak was assigned to the coupled modes between Al-O stretching and the ring deformation, and the second one, to the coupled modes between Al-O and Al-N stretching, and ring deformation [26]. In the case of the compound obtained by solid state reaction, these peaks appear at 642 cm^{-1} and 542 cm^{-1}. It is confirmed that, after the solid state reaction, the obtained compound have different configurations of the atoms.

Simulated Raman and IR spectra (in the bottom part), both indicate a double structure as can be seen also in the experimental IR spectra. Therefore the observation of doublets at these positions is strong evidence that the *mer* isomer is the predominant species in both powders. However, in the simulated IR spectra for *mer* and *fac* Alq$_3$, the strong vibration peak assigned to the coupled vibrations between Al-O and Al-N stretching, and ring deformation seems to be slightly shifted from 572 cm^{-1} to 567 cm^{-1}. The situation is quite different in the case of the coupled vibrational modes Al-O stretching and ring deformation because the shift in the simulated spectra between *mer* and *fac* Alq_3 is bigger, between 650 cm^{-1} to 680 cm^{-1}. DFT simulations allow us to identify the molecular vibrations for the calculated peak positions. For example, the vibration from 572 cm^{-1} in *mer* Alq_3 and 567 cm^{-1} in *fac* Alq_3 are assigned to the in-phase vibrations of the O-Al-N structure and those from 648 cm^{-1} and 642 cm^{-1} are assigned to the out-phase vibrations of the same structure.

3.5.Photoluminescence Analysis (PL)

The green photoluminescence (PL) of Alq_3 has been measured at room temperature using the same excitation, by means at 397 nm for the both compounds. In the case of mer-Alq_3, the green PL is peaked at 525 nm, while in the case of the pale green-yellowish compound, a blue shift up to 502 nm (0.1 eV) can be seen (figure 5). Similar behaviors concerning the blue shift photoluminescence of the Alq_3 in δ phase, was observed by M. Colle et. al [19].

Investigations of the photoluminescence excitation spectra (PLE) for our Alq_3 compound show that any excitation energy in the range of 390-425 nm contributes to the broad green photoluminescence, even if the PL is shifted between the two compounds. This behavior is due to fast non-radiative relaxations from the ${}^1B_b$ to the ${}^1L_a$ state, with subsequent radiative recombination to the ground state [27].

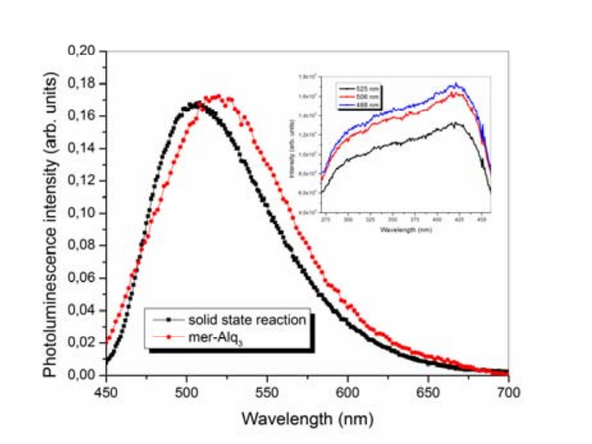

Fig. 5. Photoluminescence spectra of *mer*-Alq_3 excited at 397 nm

The PLE spectra, measured at room temperature, at different wavelengths between 488- 525 nm, can be seen in the inlet. The location of the PLE peaks is the same in the range of 275 to 450 nm. It is concluded that the PLE spectra allow better isolation and identification of different spectral contributions to the observed photo-luminescence, giving quantitative information about their ratio. From the positions of the PLE peaks, we can conclude that the broad green phosphorescence comes from the same electronic transition contributions. The blue shift of the photoluminescence in the case of our compound comes from different configurations of the atoms in the Alq$_3$.

3.6.Cathodoluminescence Analysis

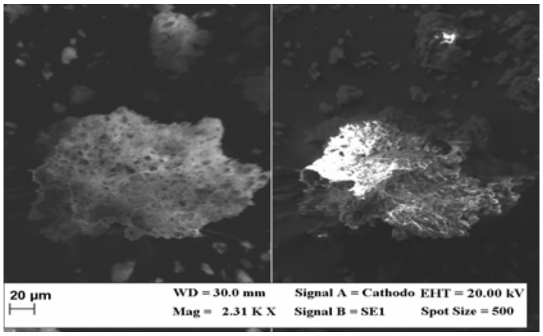

Fig. 6. Cathodoluminescence and SEM images of the solid state reaction compound.

The cathodoluminescence patterns (right side) were obtained under 20 keV electrons beams and gives useful details of the mechanism of luminescence excitation by electrons. Figure 6 shows a detailed view of cathodoluminescence image for Alq$_3$ obtained by solid state reaction and in the left side, a secondary electron image structure of the same compound. Some white spots can be seen in the secondary electron imaging suggesting a slightly charging of the Alq$_3$ surface.

It is important to note that the structure of the obtained compound is unstable under the electron beam or the X-ray generated by the LaB$_6$ cathode, even at low energy electrons, up to 5 keV. This fact can be seen during cathodoluminescence measurements.

The cathodoluminescence spectrum (CL) can be obtained by passing the emitted light under X-ray excitation through a classical monochromator and compared with the photoluminescence (PL) excited at 397 nm. Both spectra were rescaled for comparison (figure 7).

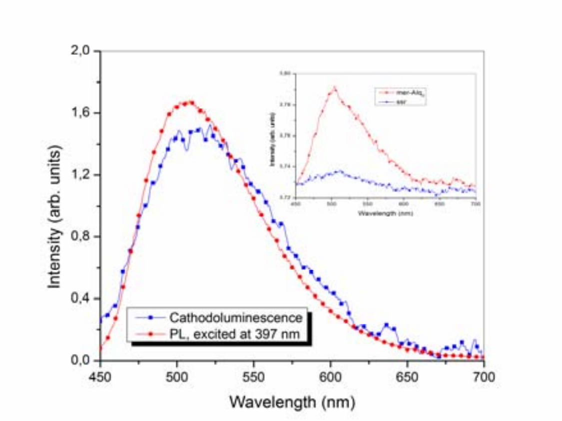

Fig. 7. Cathodoluminescence spectra of mer-Alq_3 and solid state reaction compound.

In the inlet, is shown the original cathodoluminescence spectra recorded at the same electron beam energy (20keV). It can be seen that the cathodoluminescence of our compound, is lower compared with *mer*-Alq_3 for the same excitation energy. For comparison with PL spectrum, the cathodoluminescence spectrum was recorded at low energy electron beam (5keV). This fact was explained with low efficiency of triplet state emission of 2% in the case of *fac*-Alq_3 compared with 25% in the case of *mer*-Alq_3 [29].

DFT calculations give a significant theoretical energy differences between the two Alq_3 isomers. In our case, the *mer*-Alq_3 structure is more stable, with 6.27 kcal/mol compared with fac-Alq_3, and has also different dipole lengths, 4.37 Debye and 8.9 Debye. Similar high value of 9.369 Debye for the fac-Alq_3 was also calculated [26].

Several theoretical details were obtained by Curioni, but using different functionals BYLP [30]. The energy differences between the two Alq_3 isomers was estimated at 4 kcal/mol, but other authors gives an energy differences between the two Alq_3 isomers from 4 to 8 kcal/mol [31-33].

A possible interaction between dipole moments could induce this lower energetic stability between fac-Alq_3 molecules.

4. Conclusions

A new route for Alq_3 synthesis by pure solid state reaction between $Al(OH)_3$ and 8-hydroxyquinoline was developed, the final product being a mixture between *mer* and *fac* isomers.

At 95°C, $Al(OH)_3$ is decomposed from bayerite and/or gippsite structure to boemite structure of AlO(OH) which reacts with the 8-hydroxyquinoline, leading to the Alq_3 compound.

From the XRD patterns, the crystal structure of the new compound is of low symmetry (triclinic), similar with the Alq$_3$ α-phase but with slightly differences concerning the angles and the *a*-axis which is slightly longer.

The obtained compound has lower stability suggested by the DSC and CL measurements. The cathodoluminescence is weaker than in the case of *mer*-Alq$_3$ for the same energy of the electron beam. This fact was explained with low efficiency of triplet state emission of 2% in the case of *fac*-Alq$_3$ compared with 25% in the case of *mer*-Alq$_3$. The photoluminescence of the new compound is blue shifted compared with the *mer*-Alq$_3$ with about 0.1 eV.

Vibrational spectroscopy shows some differences for those peaks which involve Al-O and Al-N bonds. This fact was evidenced by DFT calculations in which two bonds between Al-O are longest and one shorter in the case of mer-Alq$_3$ and have the same bond in the case of fac-Alq$_3$ [34].

The secondary electron images show some white spots, suggesting a slightly charging of the Alq$_3$ surface.

In particular, we examine the two molecular isomers of Alq$_3$ and argue that they could coexist in the real amorphous material, obtained by direct solid state reaction.

According to the markedly different properties we suppose that the new crystalline phase contains the facial isomer of Alq$_3$.

Acknowledgement

The work has been funded by the Sectoral Operational Programme Human Resources Development 2007-2013 of the Romanian Ministry of Labour, Family and Social Protection through the Financial Agreement POSDRU/107/1.5/S/76903.

REFERENCES

[1] *C. W. Tang and S. A. Vanslyke,* "Organic electroluminescent diodes", Appl. Phys. Lett. **vol. 51**, 1987, pp. 913.

[2] *C. W. Tang, S. A. Vanslyke and C. H.Chen,* "Electroluminescence of doped organic thin films" J. Appl. Phys., **vol. 85**, 1989, pp.3610.

[3] *S. A. Vanslyke, C. H. Chen, and C. W. Tang,* "Organic electroluminescent devices with improved stability", Appl. Phys. Lett., **vol. 69**, 1996, pp.2160.

[4] *S. Tao, P. Zhaokuai, X. Zhang, P. Wang, C. S. Lee and S. T. Lee*, "Highly Efficient Non-Doped Blue Organic Light-Emitting Diodes Based on Fluorene Derivatives with High Thermal Stability", Adv. Funct. Mater. **vol.15**, 2005, pp.1716.

[5] *K. T. Wong, Y. M. Chen, Y. T. Lin, H. C. Su and C. C. Wu*, "Nonconjugated Hybrid of Carbazole And Fluorene: A Novel Host Material for Highly Efficient Green and Red Phosphorescent OLEDs", Org. Lett., **vol.7**, 2005, pp. 5361.

[6] *G. Hughes and M. R. Bryce*, "Electron-transporting materials for organic electroluminescent and electrophosphorescent devices", J. Mater. Chem. **vol.15**, 2005, pp. 94.

[7] *A. P. Kulkarni, C. Tonzola, A. Babel and S. A. Jenekhe*, "Electron Transport Materials for Organic Light-Emitting Diodes", Chem. Mater., **vol. 16**, 2004, pp. 4556.

[8] *M. A. Baldo, D. F. O'Brien, Y. You, A. Shoustikov, S. Sibley, M. E. Thompson and S. R. Forrest*, "Highly efficient phosphorescent emission from organic electroluminescent devices", Nature, **vol.151**, 1998, pp. 395.

[9] *Y. Luo, H. Aziz, Z. D. Popovic and G. Xu*, "Electric-field-induced fluorescence quenching in dye-doped tris(8-hydroxyquinoline) aluminum layers", Appl. Phys. Lett., **vol. 89**, 2006 , pp.103-505.

[10] *M. Cölle and W. Brütting,* "Thermal, structural and photophysical properties of the organic semiconductor Alq3", Phys.Stat. Sol. (a) **vol. 201** (6), 2004, pp.1095.

[11] *M. Brinkmann, G. Gadret, M. Muccini, C. Taliani, N. Masciocchi and A. Sironi*, "Correlation between Molecular Packing and Optical Properties in Different Crystalline Polymorphs and Amorphous Thin Films of mer-Tris(8-hydroxyquinoline)aluminum(III)", J. Am. Chem. Soc. , **vol. 122**, 2000, pp. 5147.

[12] *M. Rajeswaran, T. N. Blanton, C. W. Tang, W. C. Lenhart, S. C. Switalski, D. J. Giesen, B. J. Antalek, T. D. Pawlik, D. Y. Kondakov, N. Zumbulyadis and R. H. Young*, "Structural, thermal, and spectral characterization of the different crystalline forms of Alq3, tris(quinolin-8-olato)aluminum(III), an electroluminescent material in OLED technology", Polyhedron, **vol. 28**, 2009, pp. 835.

[13] *W. A. E. Omar, H. Haverinen, O. E. O. Hormi*, "New Alq3 derivatives with efficient photoluminescence and electroluminescence properties for organic light-emitting diodes", Tetrahedron, **vol. 65**, 2009, pp. 9707.

[14] *C. H. Chen, C. W. Tang, J. Shi and K. P. Klubek*, "Recent developments in the synthesis of red dopants for Alq3 hosted electroluminescence", Thin Solid Films, **vol. 327**, 2000, pp.363.

[15] *G. S. Huang, X. L. Wu, Y. Xie, F. Kong, Z. Y. Zhang, G. G. Siu, and P. K. Chu*, "Photoluminescence from 8-hydroxy quinoline aluminum embedded in porous anodic alumina membrane", Appl. Phys. Lett. **vol. 87**, 2005, 151910.

[16] *J. J. Chiu, W. S. Wang, C. C. Kei and T. P. Perng*, “Tris-(8-hydroxyquinoline) aluminum nanoparticles prepared by vapor condensation”, App. Phys. Lett., **vol. 83**, 2003 pp.347.

[17] *J. J. Chiu, C. C. Kei, T. P. Perng and W. S. Wang*, “Organic Semiconductor Nanowires for Field Emission”, Adv. Mater., **vol. 15**, 2003, pp.1361.

[18] *M. Colle, R. E. Dinnebier and W. Brutting*, “The structure of the blue luminescent δ-phase of tris(8-hydroxyquinoline)aluminium(III) (Alq3)”, Chem. Commun., **vol. 23**, 2002,pp. 2908.

[19] *M. Colle, J. Gmeiner, W. Milius, H. Hillebrecht and W. Brutting*, “Preparation and Characterization of Blue-Luminescent Tris(8-hydroxyquinoline)-aluminum (Alq3)”, Adv.Funct. Mater., **vol.13**, 2003, pp.108.

[20] *M. Muccini, M. A. Loi, K. Kenevey, R. Zamboni, N. Masciocchi and A. Sironi*, “Blue Luminescence of Facial Tris(quinolin-8-olato)aluminum(III) in Solution, Crystals, and Thin Films”, Adv. Mater., **vol.16**, 2004, pp.861.

[21] *R. Katakura and Y. Koide*, "Configuration-Specific Synthesis of the Facial and Meridional Isomers of Tris(8-hydroxyquinolinate)aluminum (Alq3)", Inorg. Chem., **vol. 45**, 2006, pp.5730.

[22] *T. Tsuboi and Y. Torii*, “Selective Synthesis of Facial and Meridianal Isomers of Alq3”, Mol. Cryst. Liq. Cryst**, vol. 42**, 2010, pp. 529.

[23] *W. A. Rachinger*, “A correction for the α1:α2 doublet in the measurement of widths of X-ray diffraction lines”, J. Sci. Instrum., **vol. 25**, 1948, pp.254.

[24] *W. Kohn and L. J. Sham*, “Self-Consistent Equations Including Exchange and Correlation Effects”, Phys. Rev., **vol. 140**, 1965, pp. 1133.

[25] *S. V. Gabelkov, R. V. Tarasov, N. S. Poltavtsev and Y. P. Kurilo*, “Evolution of phase composition in the thermal decomposition of nanosized aluminum hydroxides”, Powder Metallurgy & Metal Ceram., **vol. 48** (7-8), 2009, pp.478.

[26] *M. D. Halls and R. Aroca*, “Vibrational spectra and structure of tris(8-hydroxyquinoline)aluminum(III)”, Can. J. Chem., **vol. 76**, 1998, pp. 1730.

[27] *G. Baldacchini, S. Gagliardi, R. M. Montereali, A. Pace and R. B. Pode*, “Optical spectroscopy of tris(8-hydroxyquinoline) aluminium thin films”, Phil. Mag. Part B, **vol. 82**(6), 2002, pp. 669.

[28] *R. J. Curry, W. P. Gillin, J. Clarkson and D. N. Batchelder*, “Morphological study of aluminum tris(8-hydroxyquinoline) thin films using infrared and Raman spectroscopy”, J. of App. Phys., **vol. 92**(4), 2002, pp. 1902.

[29] *M. Braun, J. Gmeiner, M. Tzolov, M. Coelle, F. D. Meyer, W. Milius, H. Hillebrecht, O. Wendland, J. U. von Schűtz and W. Brűtting*, “A new crystalline phase of the electroluminescent material tris(8-hydroxyquinoline) aluminum exhibiting blueshifted fluorescence”, J. of Chem. Phys., **vol. 114**(21) , 2001, pp. 9625.

[30] *A. Curioni, M. Boero and W. Andreoni*, “Alq3: ab initio calculations of its structural and electronic properties in neutral and charged states”, Chem. Phys. Lett., 1998, pp. 263-294.

[31] *Y.K. Han and S.U. Lee*, “Molecular orbital study on the ground and excited states of methyl substituted tris(8-hydroxyquinoline) aluminum(III)” Chem. Phys. Lett., **vol. 366**, 2002, pp. 9-16.

[32] *A. Curioni and W. Andreoni*, “Computer simulations for organic light-emitting diodes”, J. Res. Dev. IBM, **vol. 45**, 2001, pp. 101.

[33] *M. D. Halls and H. B. Schlegel*, ”Molecular Orbital Study of the First Excited State of the OLED Material Tris(8-hydroxyquinoline)aluminum(III)” , Chem. Mater., **vol.13**, 2001, pp. 2632.

[34] *M. Amati, F. Lelj*, “Luminescent Compounds fac- and mer-Aluminum Tris(quinolin-8-olate) A Pure and Hybrid Density Functional Theory and Time-Dependent Density Functional Theory Investigation of Their Electronic and Spectroscopic Properties”, J. Phys. Chem. A **vol. 107**, 2003 pp. 2560.